

MAPK phosphatase–3 promotes hepatic gluconeogenesis through dephosphorylation of forkhead box O1 in mice

Zhidan Wu,¹ Ping Jiao,² Xueming Huang,¹ Bin Feng,² Yajun Feng,¹ Shengyong Yang,³ Phillip Hwang,² Jing Du,² Yaohui Nie,² Guozhi Xiao,³ and Haiyan Xu²

¹Cardiovascular and Metabolism, Novartis Institutes for BioMedical Research, Cambridge, Massachusetts, USA. ²Hallett Center for Diabetes and Endocrinology, Rhode Island Hospital, Brown Medical School, Providence, Rhode Island, USA. ³Division of Hematology/Oncology, Department of Medicine, University of Pittsburgh, Pittsburgh, Pennsylvania, USA.

Insulin resistance results in dysregulated hepatic gluconeogenesis that contributes to obesity-related hyperglycemia and progression of type 2 diabetes mellitus (T2DM). Recent studies show that MAPK phosphatase–3 (MKP-3) promotes gluconeogenic gene transcription in hepatoma cells, but little is known about the physiological role of MKP-3 in vivo. Here, we have shown that expression of MKP-3 is markedly increased in the liver of diet-induced obese mice. Consistent with this, adenovirus-mediated MKP-3 overexpression in lean mice promoted gluconeogenesis and increased fasting blood glucose levels. Conversely, shRNA knockdown of MKP-3 in both lean and obese mice resulted in decreased fasting blood glucose levels. In vitro experiments identified forkhead box O1 (FOXO1) as a substrate for MKP-3. MKP-3–mediated dephosphorylation of FOXO1 at Ser256 promoted its nuclear translocation and subsequent recruitment to the promoters of key gluconeogenic genes. In addition, we showed that PPAR γ coactivator–1 α (PGC-1 α) acted downstream of FOXO1 to mediate MKP-3–induced gluconeogenesis. These data indicate that MKP-3 is an important regulator of hepatic gluconeogenesis in vivo and suggest that inhibition of MKP-3 activity may provide new therapies for T2DM.

Introduction

Insulin resistance is the underlying mechanism for the development of type 2 diabetes mellitus (T2DM). The effect of insulin in regulating glucose homeostasis is exerted through coordinated actions in multiple tissues. In the liver, insulin represses glucose output (1), while in muscle and fat, insulin stimulates glucose uptake (2, 3). In the state of insulin resistance, glucose output from the liver increases, and glucose disposal in muscle and fat decreases. Dysregulated glucose output from the liver in an insulin-resistant state contributes significantly to the development of postprandial and fasting hyperglycemia.

The liver plays a major role in providing glucose through gluconeogenesis from non-carbohydrate precursors during prolonged fasting (4). Insulin is the most important hormone for negative regulation of gluconeogenesis. In the fed state, the level of insulin rises and represses gluconeogenesis by inhibiting transcription of gluconeogenic genes (5). This effect is dependent on the lipid kinase PI3K pathway and does not require the mitogen-activated kinase cascade (6–8). Among the PI-dependent kinases, AKT has been implicated as a mediator for repressing phosphoenolpyruvate carboxykinase (*Pepck*) and *G6pase* gene expression by insulin (9, 10). Upon activation, AKT phosphorylates forkhead box O1 (FOXO1), which leads to FOXO1 nuclear exclusion and inactivation (11, 12). FOXO1 directly binds to the promoters of *Pepck* and *G6pase* genes to increase their transcription. Inactivation of FOXO1 is the major route for insulin to repress gluconeogenesis. It is not known, however, which phosphatase is responsible for the dephosphorylation and activation of FOXO1. Glucocorticoids and glucagon are major hormones

inducing expression of *Pepck* and *G6pase* genes during stress and fasting. Obesity itself constitutes a chronic stressful state and is characterized by increased production rates of cortisol (13, 14). Glucocorticoids induce gluconeogenesis through increasing transcription of gluconeogenic genes by binding to the glucocorticoid receptor. The full effect of glucocorticoids requires accessory factors such as FOXO1 and hepatocyte nuclear factor 4 α (HNF4 α) (12, 15). FOXO1 is known to increase transcription of PPAR γ coactivator 1 α (*PGC1A*), which encodes an important amplifier for hepatic gluconeogenesis (16). PGC-1 α robustly activates gluconeogenic gene expression through direct interactions with FOXO1 and HNF4 α (12, 15). Disruption of the interaction between PGC-1 α and FOXO1 by insulin represses PGC-1 α –mediated gluconeogenesis (12).

We previously identified *Mkp-3* as a top hit in an expression screen of H4IIE hepatoma cells for genes antagonizing the effect of insulin on repression of *Pepck* transcription (17). MKP-3 and glucocorticoids synergistically activated *PEPCK* transcription and increased gluconeogenesis in vitro. Despite these findings in vitro, the role of MKP-3 in regulation of glucose metabolism and the underlying mechanism remain to be elucidated. The only known substrates for MKP-3 are ERKs, which do not play a significant role in mediating the inhibitory effect of insulin on gluconeogenesis. Thus, MKP-3 may regulate gluconeogenesis through other unknown substrates besides ERKs. In this study, we investigated the role of MKP-3 in regulating energy homeostasis in animals. In addition, we dissected the molecular mechanism by which MKP-3 regulates hepatic gluconeogenesis. Our findings demonstrate that MKP-3 is an important regulator of glucose metabolism and provide insight into the mechanism by which MKP-3 regulates the expression of gluconeogenic genes and hepatic glucose production.

Conflict of interest: The authors have declared that no conflict of interest exists.

Citation for this article: *J Clin Invest.* 2010;120(11):3901–3911. doi:10.1172/JCI43250.

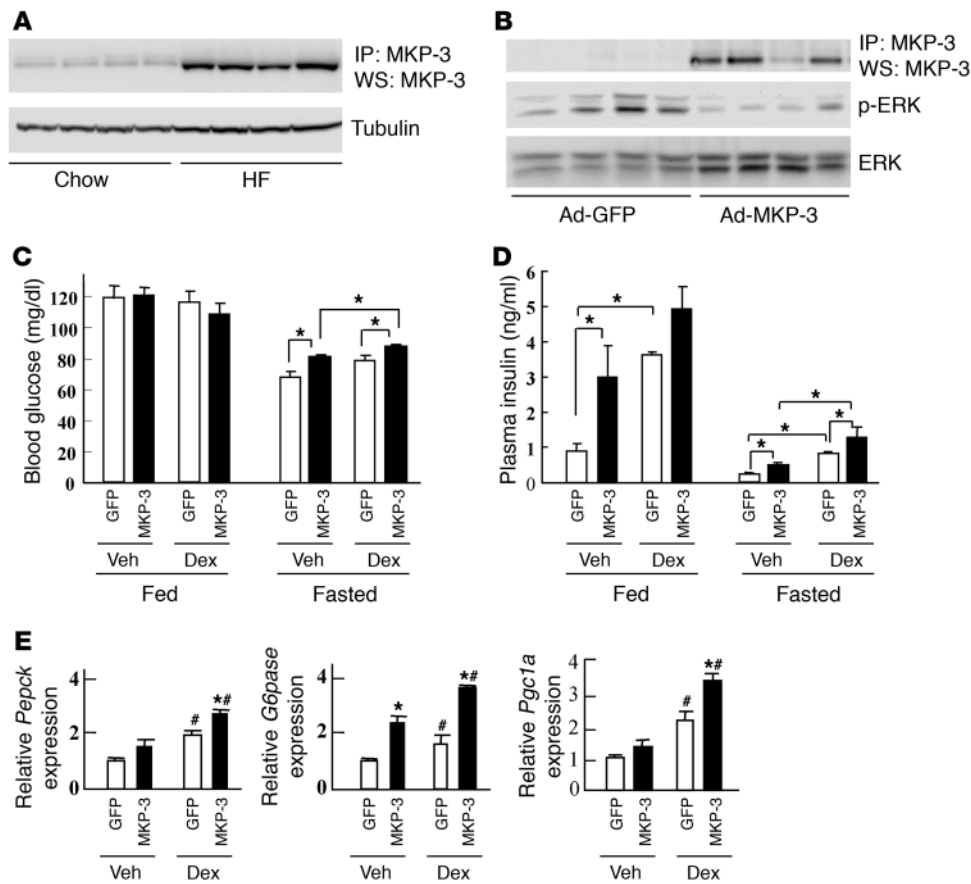


Figure 1 Overexpression of MKP-3 in lean mice. (A) Endogenous MKP-3 protein levels are increased in the liver of DIO mice. MKP-3 was immunoprecipitated from liver lysates using the Exactra D system to remove IgG signals, and MKP-3 protein was detected by Western blot analysis (WS) ($n = 4$). Loading was indicated with tubulin content in these samples. (B) MKP-3 protein in the liver of lean mice injected with adenoviruses expressing GFP or MKP-3 ($n = 4$). Phospho-ERK was examined as a functional readout of MKP-3 overexpression. (C) Blood glucose levels in lean mice expressing GFP or MKP-3 ($n = 3-14$). * $P < 0.05$. (D) Plasma insulin levels in lean mice overexpressing GFP or MKP-3 ($n = 3-6$). * $P < 0.05$, MKP-3-overexpressing versus GFP-overexpressing mice. (E) Relative expression of *Pepck*, *G6pase*, and *Pgc1a* genes in the liver of fasted lean mice injected with adenoviruses expressing GFP or MKP-3 ($n = 3-6$). * $P < 0.05$, MKP-3 versus GFP; # $P < 0.05$, Dex versus vehicle.

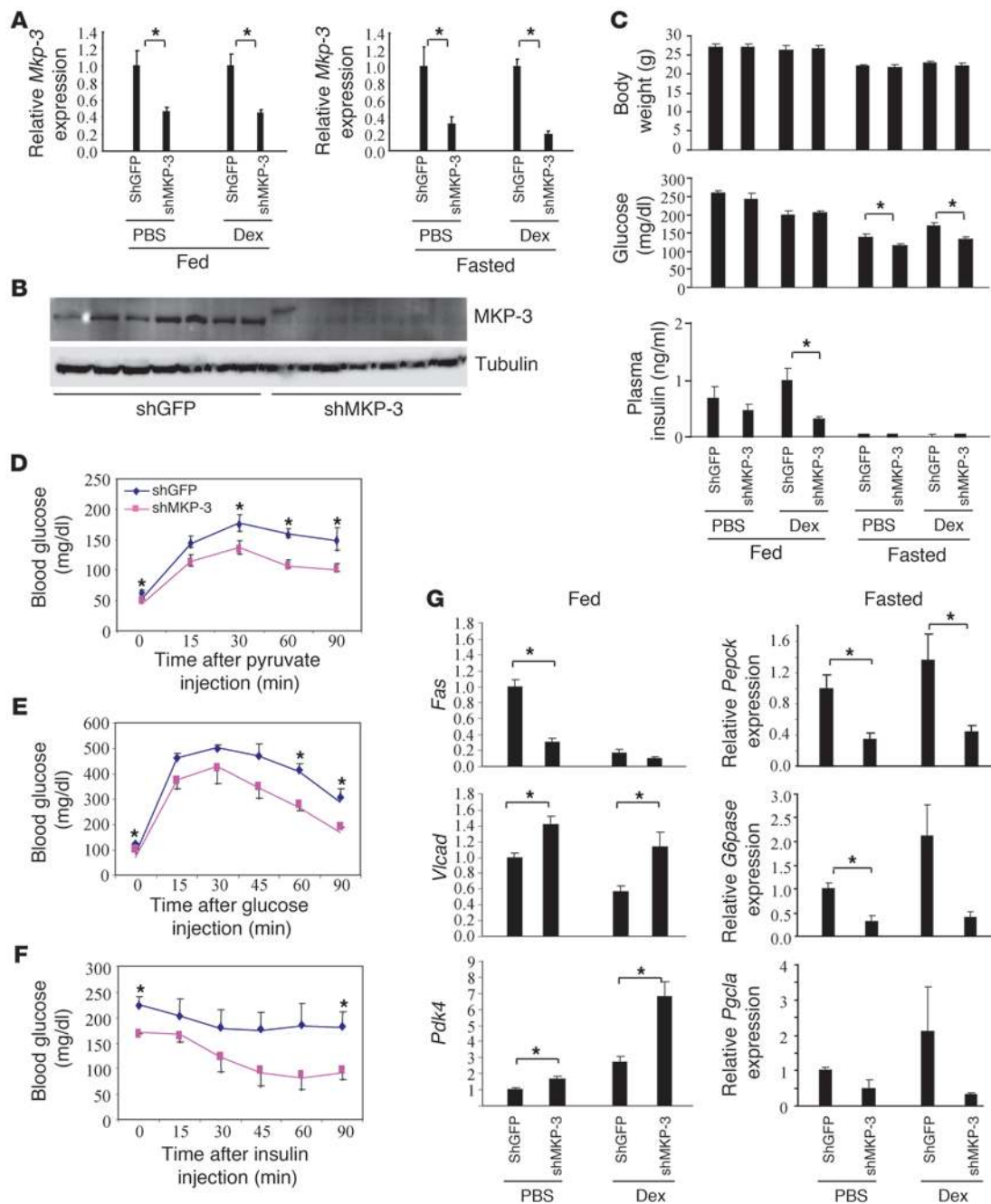
Results

MKP-3 overexpression increases fasting blood glucose levels in lean mice. Originally screened from a cDNA library derived from *ob/ob* mice, MKP-3 was identified as a top candidate for antagonizing the repressive effect of insulin on *Pepck* transcription in cultured hepatoma cells (17). The only known literature regarding the role of MKP-3 in metabolism showed that it promotes gluconeogenesis in hepatoma cells by an unknown mechanism (17). Here, the potential role of MKP-3 in whole body energy homeostasis is studied for the first time to our knowledge. MKP-3 protein levels in the livers of diet-induced obese (DIO) mice were significantly increased (Figure 1A), suggesting that MKP-3 may play a role in dysregulated liver gluconeogenesis during an insulin-resistant state. Interestingly, expression of MKP-3 protein could be regulated by hormones controlling blood glucose levels. In the livers of lean mice 1 hour after injection, glucagon acutely upregulated MKP-3 protein expression, which decreased 5 hours after injection (Supplemental Figure 1A; supple-

mental material available online with this article; doi:10.1172/JCI43250DS1). In contrast, the effect of insulin on suppressing MKP-3 protein expression occurred more slowly, requiring 20 hours after injection (Supplemental Figure 1B). To investigate the role of MKP-3 on glycemic control in vivo, we first overexpressed MKP-3 in the liver of lean mice via adenovirus-mediated gene transfer. Overexpression of MKP-3 in the liver of lean mice significantly decreased phosphorylation of ERK1/2, the only known direct target of MKP-3 (Figure 1B). Our previous study with hepatoma cells revealed that dexamethasone (Dex) markedly potentiates MKP-3-induced *Pepck* transcription. Dex was therefore injected into MKP-3-overexpressing mice. In the fed state, MKP-3 overexpression did not have an effect on blood glucose levels (Figure 1C) or expression of gluconeogenic genes (data not shown) but significantly increased plasma insulin levels in vehicle-treated mice compared with mice expressing a GFP control (Figure 1D), indicating insulin resistance. In the fasted state, MKP-3 overexpression significantly increased blood glucose and plasma insulin levels in both vehicle- and Dex-treated animals (Figure 1, C and D). Only *G6pase* gene expression was significantly increased by MKP-3 overexpression in vehicle-treated mice, while expression levels of *Pepck*, *G6pase*, and *Pgc1a* genes were all significantly increased by MKP-3

overexpression in Dex-treated animals (Figure 1E). These results indicate that overexpression of MKP-3 promotes hepatic gluconeogenesis in vivo and this effect is further enhanced by Dex. Overexpression of MKP-3 in isolated primary hepatocytes also showed increased gluconeogenic gene expression and elevated glucose output (Supplemental Figure 2). These results indicate that elevation of MKP-3 expression in obesity may contribute to the pathogenesis of insulin resistance and hyperglycemia.

Reduction of hepatic MKP-3 expression lowers fasting blood glucose levels in both lean and obese mice. To investigate the role of endogenous MKP-3 in hepatic glucose metabolism, expression of MKP-3 was knocked down in the liver of lean mice by adenovirus-mediated expression of short hairpin interfering RNA (shRNA) targeting mouse MKP-3. *MKP-3* mRNA levels were reduced by 54%–56% in the fed state and 68%–83% in the fasted state in both PBS- and Dex-treated mice (Figure 2A), while MKP-3 protein levels were barely detectable (Figure 2B). Reduction of MKP-3 did not affect body

**Figure 2**

MKP-3 knockdown in lean mice. Male C57BL/6J mice were injected with adenoviruses expressing either shGFP or shMKP-3. A subgroup of the mice were injected with Dex at a dose of 15 mg/kg. (A) Relative *MKP-3* mRNA levels in lean mice injected with Ad-shGFP or Ad-shMKP-3 in the fed or fasted condition with or without Dex ($n = 5-7$ each group). (B) MKP-3 protein expression in lean mice injected with Ad-shGFP or Ad-shMKP-3 in the fasted condition ($n = 7$ each group). (C) Body weight, blood glucose, and plasma insulin levels in lean mice injected with Ad-shGFP or Ad-shMKP-3 in fed or fasted condition with or without Dex ($n = 5-7$ each group). (D) Pyruvate tolerance test ($n = 6$ each group). (E) Glucose tolerance test ($n = 4-5$ each group). (F) Insulin tolerance test ($n = 4-5$ each group). (G) Gene expression analysis of lean mice with reduced hepatic MKP-3 expression. * $P < 0.05$, mice injected with Ad-shGFP versus mice injected with Ad-shMKP-3.

weight but significantly reduced fasting blood glucose levels by 17% in lean mice injected with PBS and by 21% in lean mice injected with Dex (Figure 2C). The decreased expression of MKP-3 also lowered plasma insulin levels in lean mice in the fed state, and the difference was statistically significant in lean mice injected with

Dex (Figure 2C). To examine whether decreased MKP-3 expression attenuates the gluconeogenic capacity of mice in response to a load of gluconeogenic precursor, we injected pyruvate. Pyruvate challenge in the lean mice resulted in significant decreases in blood glucose levels at 0, 30, 60, and 90 minutes in mice injected with

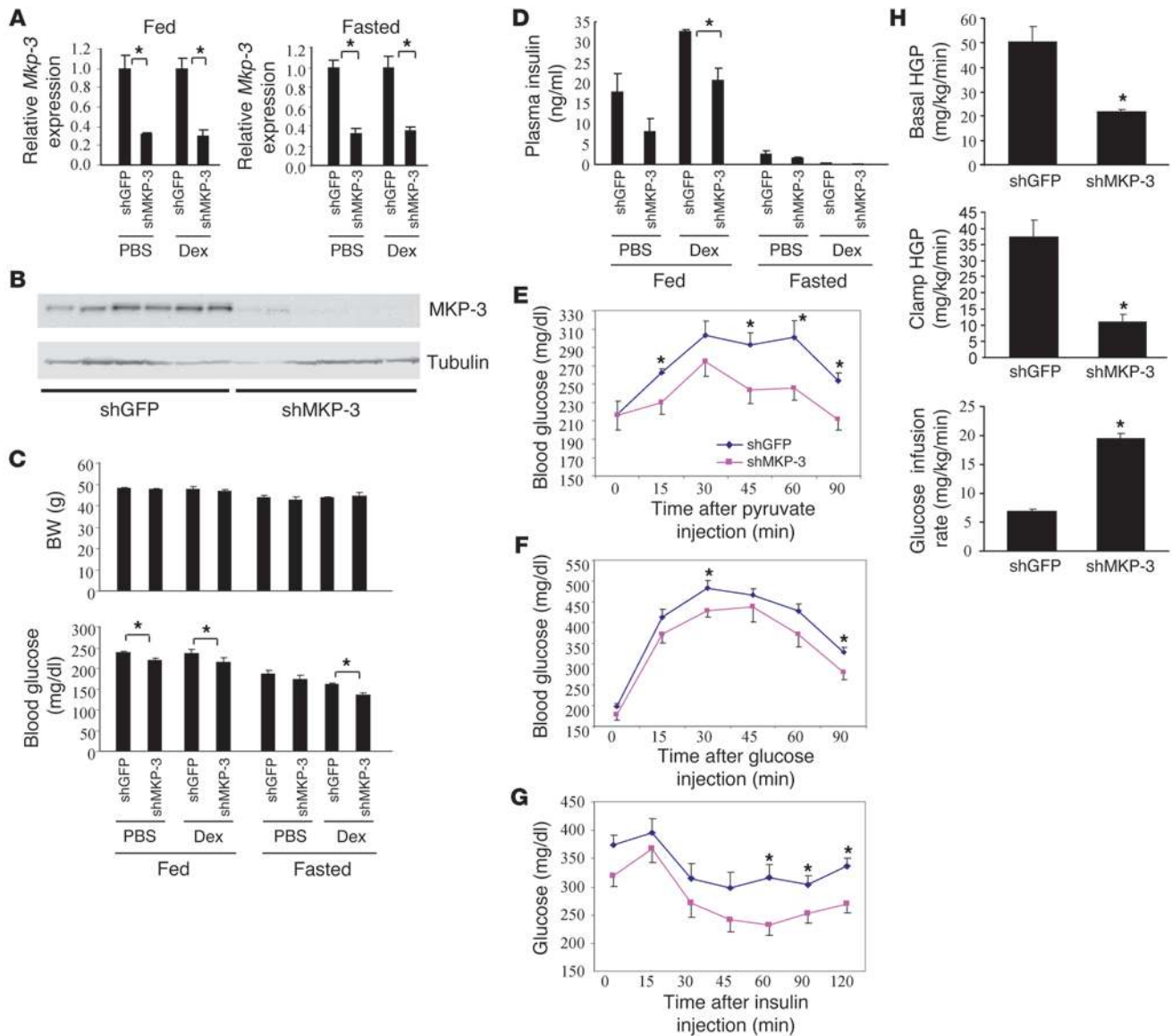


Figure 3

MKP-3 knockdown in DIO mice. Male C57BL/6J DIO mice were injected with adenoviruses expressing either shGFP or shMKP-3. A subgroup of the mice were injected with Dex at a dose of 15 mg/kg. (A) Relative *Mkp-3* mRNA levels in DIO mice injected with Ad-shGFP or Ad-shMKP-3 in the fed or fasted condition with or without Dex ($n = 5-6$ each group). (B) MKP-3 protein expression in DIO mice injected with Ad-shGFP or Ad-shMKP-3 ($n = 6$ each group). (C) Body weight and blood glucose levels in DIO mice injected with Ad-shGFP or Ad-shMKP-3 in the fed or fasted condition with or without Dex ($n = 5-7$ each group). (D) Insulin levels in DIO mice injected with Ad-shGFP or Ad-shMKP-3 in the fed or fasted condition with or without Dex ($n = 5-7$ each group). (E) Pyruvate tolerance test ($n = 6$ each group). (F) Glucose tolerance test ($n = 6$ each group). (G) Insulin tolerance test ($n = 7$ each group). (H) Hyperinsulinemic-euglycemic clamp study ($n = 3$ each group). HGP, hepatic glucose production. * $P < 0.05$, mice injected with Ad-shGFP versus mice injected with Ad-shMKP-3.

adenoviruses expressing shMKP-3 compared with control mice injected with adenoviruses expressing shGFP (Figure 2D). This result indicates that mice with reduced hepatic MKP-3 expression have significantly decreased gluconeogenic capacity in response to a challenge with a gluconeogenic precursor. Glucose tolerance tests revealed that reduced MKP-3 expression in the liver of lean mice improved glucose tolerance (Figure 2E), while insulin tolerance test demonstrated enhanced systemic insulin sensitivity (Figure 2F). Gene expression analysis indicated that reduced MKP-3 expression in the liver of lean mice not only reduced expression of

gluconeogenic genes (*Pepck*, *G6pase*, and *Pgc1a*) but also decreased expression of lipogenic genes such as *Fas* (Figure 2G). In addition, MKP-3 knockdown increases expression of *Vlcad*, which is involved in fatty acid oxidation, and *Pdk4*, which is a negative regulator of glucose oxidation (Figure 2G). These results suggest that the impaired gluconeogenic capacity in lean mice caused by reduced hepatic MKP-3 expression may shift the energy source from glucose utilization to fatty acid utilization.

Since MKP-3 expression is significantly increased in the liver of obese mice, we then explored whether reduction of MKP-3 in the

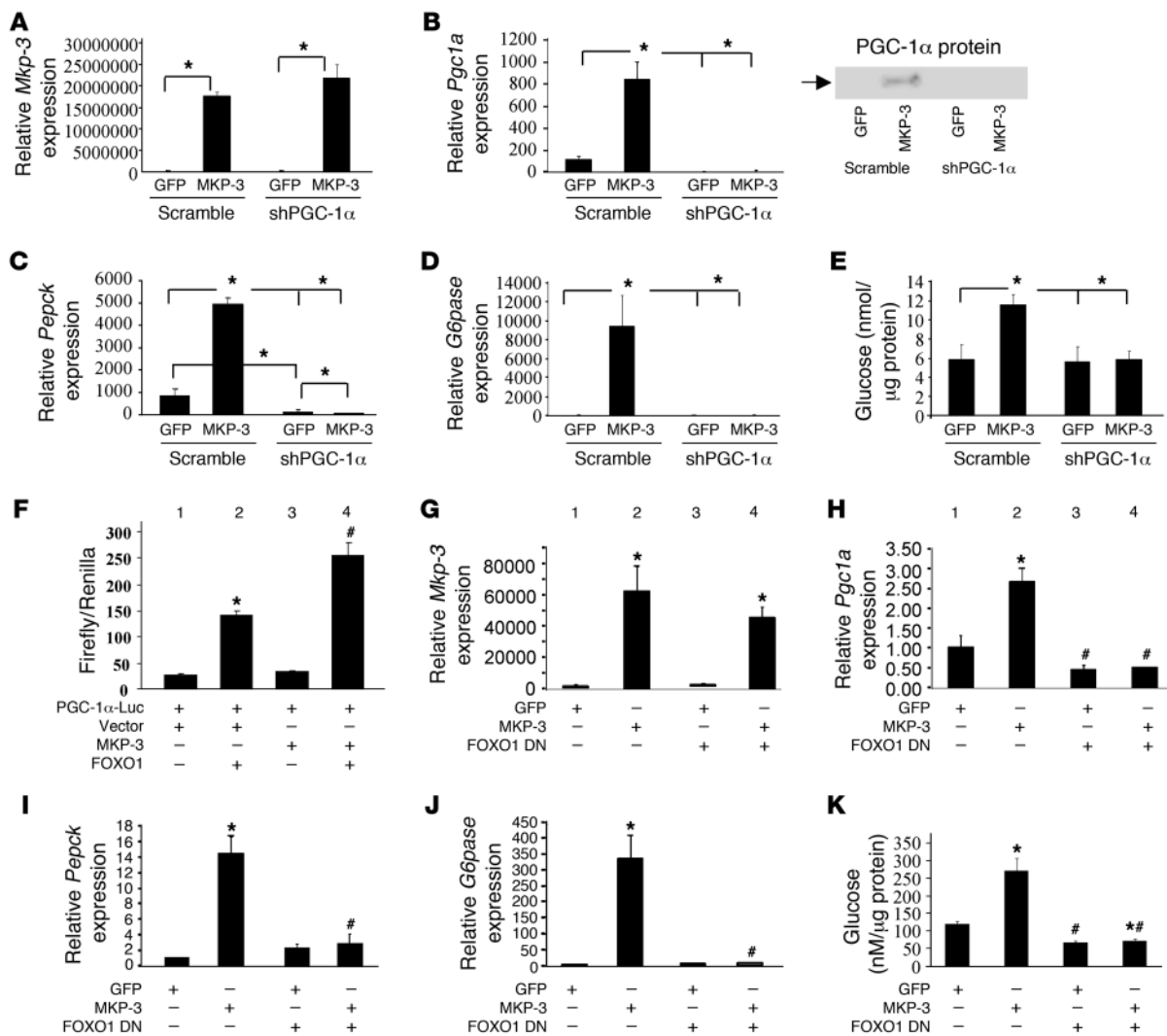


Figure 4

PGC-1α and FOXO1 are required for MKP-3-induced gluconeogenesis. (A–E) Effect of PGC-1α knockdown on MKP-3-induced gluconeogenesis. MKP-3 or GFP is coexpressed with PGC-1α shRNA in rat primary hepatocytes via adenovirus-mediated gene transfer. Expression of *Mkp-3* (A), *Pgc1a* (B), *Pepck* (C), and *G6pase* (D) genes as well as glucose output (E) were measured. **P* < 0.05, MKP-3-overexpressing versus GFP-overexpressing cells in the presence/absence of PGC-1α shRNA. (F) MKP-3 and FOXO1 have an additive effect on *Pgc1a* transcription. The 2-kb *Pgc1a* promoter-driven luciferase construct was cotransfected with vector control or MKP-3 expression plasmid in the presence/absence of FOXO1. (G–K) Effect of dominant-negative (DN) FOXO1 Δ256 overexpression on MKP-3-induced gluconeogenesis. MKP-3 or GFP was coexpressed with FOXO1 Δ256 in rat primary hepatocytes via adenovirus-mediated gene transfer. Expression of *Mkp-3* (G), *Pgc1a* (H), *Pepck* (I), and *G6pase* (J) genes as well as glucose output (K) were measured. **P* < 0.05, bar 2 versus 1; bar 4 versus 3; #*P* < 0.05, bar 3 versus 1; bar 4 versus 2.

liver of obese mice has any effect on glycemic control. Two rodent obesity models, DIO and *ob/ob* mice, were used for these experiments. In DIO mice, *Mkp-3* mRNA levels were significantly reduced by 68%–70% in the fed condition and 65%–68% in the fasted state (Figure 3A). Protein expression levels were consistent with mRNA levels (Figure 3B). Reduction of MKP-3 expression in the liver of DIO mice decreased blood glucose levels in both fed and fasted states without affecting body weight (Figure 3C). Plasma insulin levels were lower in DIO mice with reduced hepatic MKP-3 expression, and the difference reached statistical significance in the fed condition in mice injected with Dex (Figure 3D). DIO mice with reduced hepatic MKP-3 expression had an impaired response to a pyruvate challenge (Figure 3E). Glucose tolerance tests showed that MKP-3 knockdown

in the liver of DIO mice improved glucose tolerance (Figure 3F). Improved systemic insulin sensitivity was indicated by an insulin tolerance test (Figure 3G). Most importantly, a hyperinsulinemic-euglycemic clamp study demonstrated decreased basal and clamp hepatic glucose production but increased glucose infusion rate in DIO mice with reduced hepatic MKP-3 expression (Figure 3H). Gene expression analysis revealed that hepatic MKP-3 knockdown in DIO mice reduced expression of *Pepck* and *Fas* but increased expression of *Vldlr* and *Pdk4* genes (Supplemental Figure 3).

The MKP-3 knockdown study was also performed in genetically obese *ob/ob* mice. *Mkp-3* expression was significantly reduced by 80% at the mRNA level (Supplemental Figure 4A), and protein levels were barely detectable (Supplemental Figure 4B). Reduction of

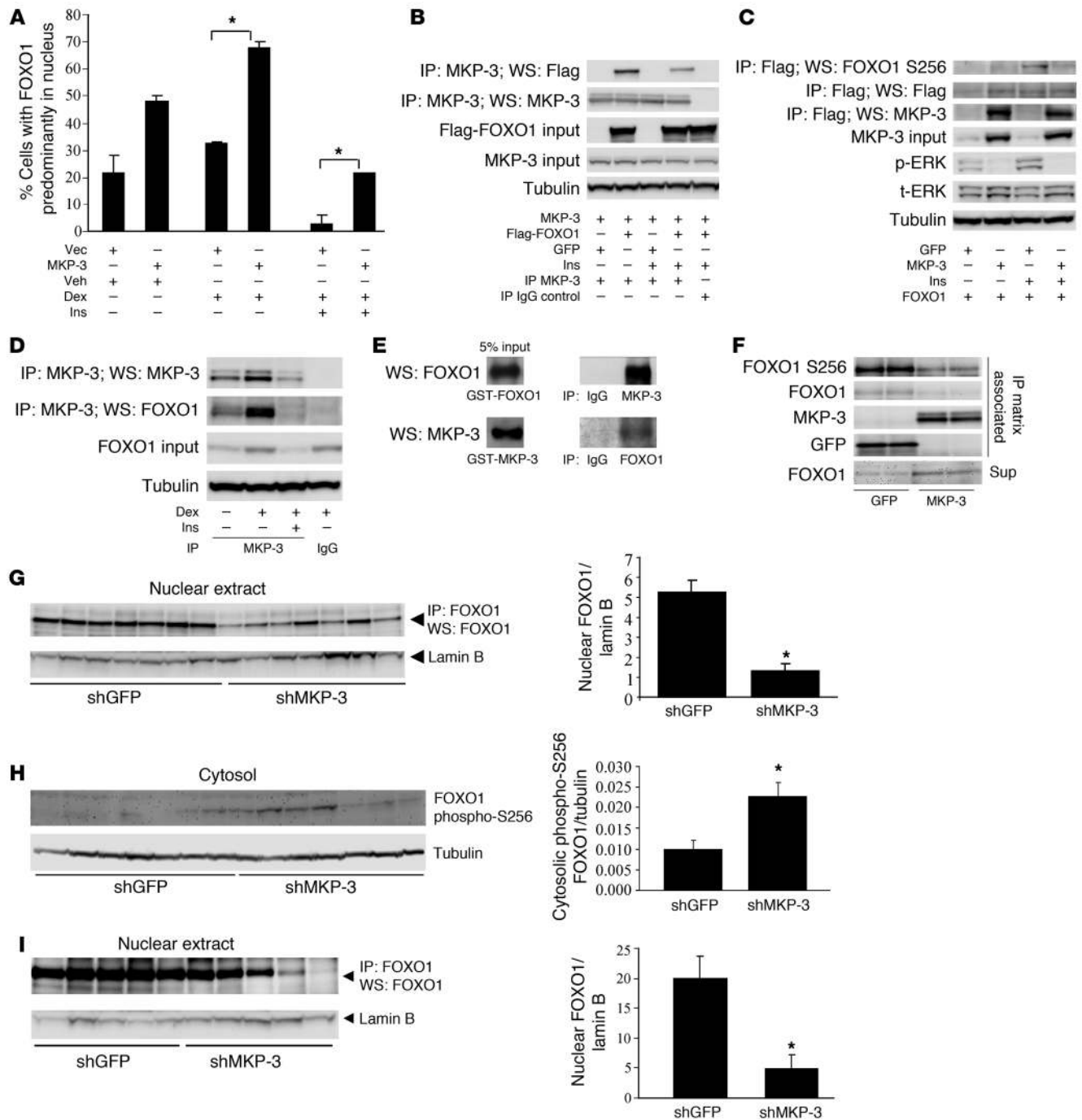
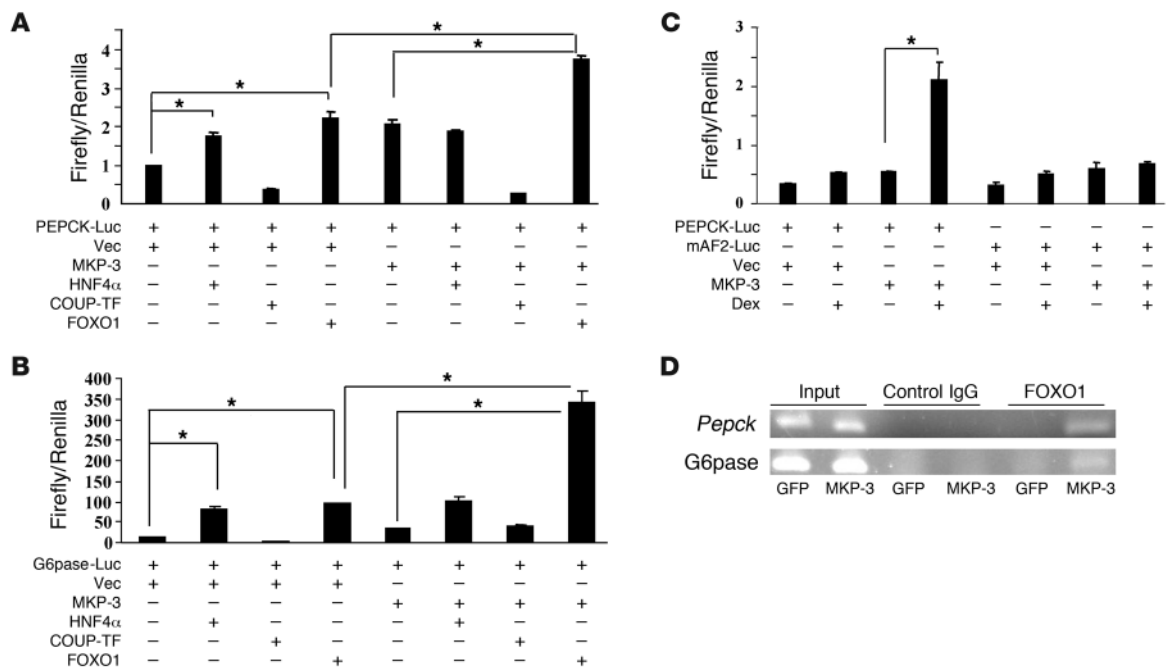


Figure 5

FOXO1 is a substrate and downstream mediator of MKP-3. (A) Effect of MKP-3 overexpression on FOXO1 nuclear translocation. (B) Co-immunoprecipitation of MKP-3 and Flag-FOXO1 in overexpression study. (C) Effect of MKP-3 overexpression on Flag-FOXO1 phosphorylation. (D) Co-immunoprecipitation of endogenous MKP-3 and FOXO1. (E) GST-pull-down study. (F) In vitro dephosphorylation of endogenous FOXO1 immunoprecipitated from insulin-stimulated Fao cells by MKP-3. (G) Nuclear FOXO1 content in lean mice injected with Ad-shGFP or Ad-shMKP-3 in the fasted condition ($n = 7$ each group). (H) Cytosolic FOXO1 Ser256 phosphorylation in mice as described in G. (I) Nuclear FOXO1 content in DIO mice injected with Ad-shGFP or Ad-shMKP-3 in the fasted condition ($n = 5$ each group). * $P < 0.05$, MKP-3-overexpressing versus vector-overexpressing cells. Ins, insulin; Vec, vector.

hepatic MKP-3 expression did not affect body weight but significantly reduced fasting blood glucose level, by 22%, in *ob/ob* mice (Supplemental Figure 4C). Experiments performed in isolated primary hepatocytes showed consistent results; MKP-3 knockdown

was associated with decreased gluconeogenic gene expression and lowered glucose output (Supplemental Figure 5). These results indicate that MKP-3 plays an important role in glycemic control in vivo and in obese and insulin-resistant states.

**Figure 6**

MKP-3 potentiates the effect of FOXO1 on transcription of gluconeogenic genes. (A and B) Additive effect between MKP-3 and FOXO1 on transcription of *Pepck* and *G6pase* promoters. (C) Effect of AF2 mutation on MKP-3-promoted *Pepck* transcription. (D) MKP-3 recruits endogenous FOXO1 into the promoters of endogenous *Pepck* and *G6pase* genes. * $P < 0.05$.

PGC-1 α is required for MKP-3-induced gluconeogenesis in primary hepatocytes. To explore the molecular mechanism underlying MKP-3-induced gluconeogenic gene expression and glucose output, we first examined whether PGC-1 α , a key gluconeogenic transcription coactivator, is regulated by MKP-3. Primary hepatocytes were transduced with adenoviruses to overexpress MKP-3 and/or knock down PGC-1 α . As shown in Figure 4A, *Mkp-3* mRNA levels were greatly elevated in cells transduced with adenoviruses expressing MKP-3. The *Pgc1 α* mRNA level was markedly increased by MKP-3 overexpression, and this induction was prevented when cells were transduced with the PGC-1 α shRNA adenovirus (Figure 4B). In addition, the increase in *Pepck* and *G6pase* mRNA levels by MKP-3 overexpression were completely abolished when PGC-1 α was knocked down (Figure 4, C and D). Furthermore, PGC-1 α knock-down completely abolished the MKP-3-mediated increase in glucose output in rat primary hepatocytes (Figure 4E). These results indicate that MKP-3-induced gluconeogenesis requires PGC-1 α .

MKP-3 increases PGC-1 α transcription and gluconeogenesis via FOXO1. Since MKP-3-mediated gluconeogenesis requires PGC-1 α , we further investigated how MKP-3 regulates PGC-1 α expression. To evaluate whether MKP-3 increases transcription of *Pgc1 α* , a 2-kb *Pgc1 α* promoter-driven luciferase construct was cotransfected with MKP-3 or a vector control. Overexpression of MKP-3 alone did not increase *Pgc1 α* transcription, suggesting that additional factor(s) are required for the induction of PGC-1 α expression by MKP-3 (Figure 4F, bar 3 vs. 1). FOXO1 has been shown to activate *PGC1A* transcription and promotes gluconeogenesis (16). To test whether FOXO1 mediates MKP-3-induced *Pgc1 α* transcription, *Pgc1 α* promoter luciferase reporter and FOXO1 were cotransfected into Fao cells along with MKP-3 or a vector control. As previously reported, FOXO1 alone increased *Pgc1 α* transcription, which was further

enhanced by MKP-3 (Figure 4F, lane 4 vs. 2). These data indicate that MKP-3 overexpression increases endogenous PGC-1 α expression through an indirect mechanism, possibly through modulation of FOXO1 activity. To determine the role of endogenous FOXO1 in MKP-3-induced PGC-1 α expression and gluconeogenesis, MKP-3 was coexpressed with a dominant-negative FOXO1 $\Delta 256$ construct in primary hepatocytes via adenovirus-mediated gene transfer. As expected, overexpression of MKP-3 significantly increased the expression of *Pgc1 α* , *Pepck*, and *G6pase* genes, as well as elevating glucose production (Figure 4, G-K). FOXO1 $\Delta 256$ completely abolished MKP-3-induced expression of *Pgc1 α* , *Pepck*, and *G6pase* genes (Figure 4, H-J). MKP-3-induced glucose output was also blunted by inhibition of FOXO1 (Figure 4K). In addition, we knocked down expression of endogenous FOXO1 by interfering RNA in primary hepatocytes and observed similar results. Endogenous *Foxo1* mRNA levels were reduced by 55%–66%, which was sufficient to significantly reduce expression of gluconeogenic genes and decrease glucose output in primary hepatocytes (Supplemental Figure 6). These results indicate FOXO1 as an essential mediator of MKP-3-stimulated PGC-1 α expression and gluconeogenic program.

MKP-3 enhances FOXO1 transcriptional activity via dephosphorylation of FOXO1. The results shown in Figure 4 indicate that MKP-3-induced gluconeogenesis requires both FOXO1 and PGC-1 α , with FOXO1 acting upstream of PGC-1 α . We speculated that MKP-3 increases *Pepck* and *G6pase* gene expression through increased FOXO1 activity by FOXO1 dephosphorylation, which promotes its nuclear translocation. To test this hypothesis, we first examined whether MKP-3 overexpression could reduce insulin signaling through dephosphorylation of IR, IRS-1, and Akt, which could reduce FOXO1 phosphorylation and subsequently promote its nuclear translocation. There were no differences in the levels of

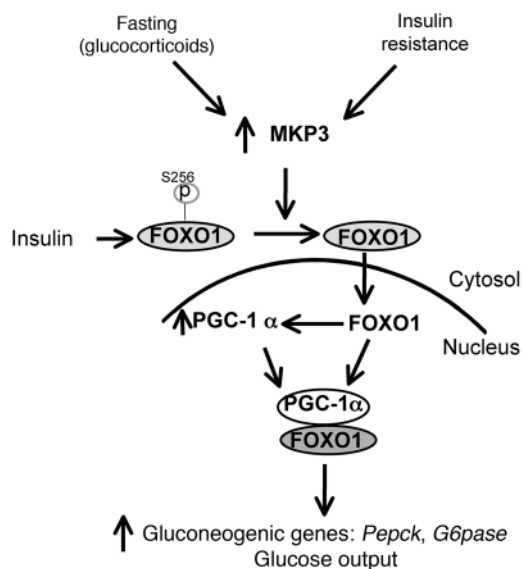


Figure 7
Model illustrating the working hypothesis of MKP-3-induced gluconeogenesis. Increased expression of MKP-3, induced either by glucocorticoids or insulin-resistant state such as obesity, will decrease phosphorylation of FOXO1 on Ser256, which subsequently promotes FOXO1 translocation from cytosol to nucleus. Activated FOXO1 increases transcription of *Pgc1a* and also interacts with PGC-1 α to initiate the gluconeogenic program.

insulin-stimulated phosphorylation of IR, IRS-1, and Akt between cells overexpressing MKP-3 and cells overexpressing GFP (Supplemental Figure 7A). However, MKP-3 overexpression stimulated FOXO1 nuclear translocation under both basal and Dex-stimulated conditions (Figure 5A and Supplemental Figure 7B). Insulin suppressed FOXO1 nuclear translocation in both control cells and MKP-3-overexpressing cells but partial antagonization was observed in the presence of excessive amounts of MKP-3 (Figure 5A). FOXO1 nuclear translocation is a step necessary for FOXO1 to bind to the promoters of gluconeogenic genes. To determine the mechanism of MKP-3-promoted FOXO1 nuclear translocation and explore the possibility that FOXO1 is a novel substrate for MKP-3, we examined the potential interaction between MKP-3 and FOXO1. MKP-3 and Flag-FOXO1 or GFP were coexpressed in Fao cells. Flag-FOXO1 was detected in the MKP-3 immunoprecipitation complex but not in the IgG IP control and vice versa (Figure 5, B and C). Insulin-stimulated phosphorylation of FOXO1 on the N-terminal Akt site (Thr24) and the Akt site located in the forkhead domain (Ser256) are critical for retaining FOXO1 in the cytosol and maintaining its association with 14-3-3 protein (18). To examine the effect of MKP-3 on insulin-stimulated phosphorylation on Thr24 and Ser256 of FOXO1, we coexpressed MKP-3 and Flag-FOXO1 in Fao cells at a ratio of 5:1. ERKs are the only known substrates for MKP-3, and their phosphorylation status was examined to confirm the established function of MKP-3. Overexpression of MKP-3 reduced ERK phosphorylation to a barely detectable level (Figure 5C). Importantly, overexpression of MKP-3 decreased insulin-stimulated FOXO1 phosphorylation on Ser256 in Fao cells (Figure 5C). Endogenous FOXO1 could also be detected on the same blot loaded with endogenous MKP-3 immunoprecipitation complex but not in the IgG IP control (Figure 5D), indicating that MKP-3

and FOXO1 exist in the same protein complex under physiologically relevant conditions. The interaction between endogenous MKP-3 and FOXO1 was enhanced by Dex but reduced by insulin (Figure 5D). A GST pull-down study demonstrated that MKP-3 and FOXO1 could directly interact with each other in vitro (Figure 5E). When immunoprecipitated MKP-3 or GFP was incubated with immunoprecipitated FOXO1 prepared from insulin-stimulated Fao cells, the presence of MKP-3 reduced FOXO1 phosphorylation on Ser256 (Figure 5F). Although immunoprecipitation matrix-associated FOXO1 was also reduced in the presence of MKP-3, this was most likely due to release of unphosphorylated FOXO1 into the reaction buffer (Figure 5F). Data from in vivo experiments also confirmed that MKP-3 regulates FOXO1 nuclear translocation and phosphorylation. Nuclear FOXO1 content was significantly decreased and cytosolic FOXO1 phosphorylation on Ser256 was significantly increased in the liver of lean mice upon MKP-3 knock-down (Figure 5, G and H). Decreased nuclear FOXO1 content was also observed in DIO mice injected with shMKP-3 virus (Figure 5I), indicating decreased gluconeogenic capacity. These results support the hypothesis that FOXO1 is a substrate for MKP-3.

To investigate whether MKP-3 enhances FOXO1 and/or other accessory factors in inducing transcription of gluconeogenic genes, a *Pepck* promoter-driven luciferase vector was cotransfected with HNF4 α , chicken ovalbumin upstream promoter transcription factor (COUP-TF), or FOXO1 into Fao cells in the presence/absence of MKP-3. Both HNF4 α and FOXO1 significantly increased transcription of *Pepck* in the absence of MKP-3. MKP-3 enhanced FOXO1-activated but had no effect on HNF4 α -induced *Pepck* transcription (Figure 6A). Similar results were observed with the *G6pase* promoter (Figure 6B). Mutations in the FOXO1-binding AF2 element of the *Pepck* promoter diminished the synergistic effect of MKP-3 with Dex to activate transcription of the *Pepck* promoter (Figure 6C). Chip assays provided further evidence that MKP-3 promotes recruitment of endogenous FOXO1 to the promoters of endogenous *Pepck* and *G6pase* genes (Figure 6D). These results suggest that MKP-3-promoted gluconeogenesis is mediated at least in part by its phosphatase activity toward dephosphorylating Ser256 of FOXO1, thereby activating FOXO1 and subsequently increasing its nuclear translocation. CRTC2, a transcriptional coactivator of CREB required for initiating the gluconeogenic program, was also explored as a possible mediator of MKP-3-promoted gluconeogenesis. CRTC2 and MKP-3 did not have any significant additive effects in activating *Pepck* and *G6pase* promoters, suggesting that CRTC2 is not likely a downstream target of MKP-3 (Supplemental Figure 8).

Discussion

Abnormal hepatic glucose output contributes substantially to obesity-related T2DM. MKP-3 is a dual-specificity phosphatase that plays an important role in attenuation of MAPK signaling. Activation of the Ras/Raf/MEK/ERK pathway can partially inhibit *Pepck* expression and is sufficient to mediate the suppression of *G6pase* gene expression by PMA. Both effects are independent of insulin action (7, 19). Interestingly, mice deficient in the signaling adapter p62 exhibit increased basal ERK activity and decreased expression of *Pgc1a* and *Pepck* genes in the liver despite an overall obese and insulin-resistant phenotype (20). However, activation of the ERK pathway is not required for repression of *Pepck* and *G6pase* gene expression by insulin (7, 8).

We previously reported that MKP-3 could antagonize the effect of insulin on repressing gluconeogenesis in cultured Fao hepatoma



cells (17). In this study, we investigated the role of MKP-3 in hepatic glucose metabolism in whole animals and dissected the underlying molecular mechanism. The results from these studies demonstrate, for the first time to our knowledge, a critical role of MKP-3 in regulating energy homeostasis in vivo. Expression of MKP-3 was elevated in both genetically and diet-induced obese mice. In our previous report, we examined MKP-3 protein level by direct immunoblot analysis and found that MKP-3 was significantly increased in the liver of *ob/ob* mice but only trended upward in DIO mice fed a high-fat diet with 45% calories derived from fat compared with control mice fed a chow diet with 10% calories derived from fat (17). In this study, we reexamined MKP-3 protein levels in the liver of DIO mice fed a high-fat diet with 60% calories derived from fat compared with control mice fed a chow diet with 5% calories derived from fat (the latter DIO model exhibits a higher degree of adiposity) by immunoprecipitation and demonstrated that MKP-3 protein was significantly increased. MKP-3 overexpression in the livers of lean mice significantly increased fasting blood glucose levels and postprandial insulin levels. Adenovirus-mediated interfering RNA knockdown of hepatic MKP-3 expression in lean mice significantly reduced fasting blood glucose levels and improved systemic insulin sensitivity. Most importantly, reduction of MKP-3 expression in both diet-induced and genetically obese mice alleviated hyperglycemia. Elevation of hepatic MKP-3 expression in the insulin-resistant state may contribute to the inappropriate activation of gluconeogenesis in type 2 diabetes. Our results demonstrate that MKP-3 is an important regulator of hepatic gluconeogenesis in vivo.

In addition to demonstrating a role for MKP-3 in glucose homeostasis in vivo, we also explored the underlying molecular mechanism using primary and cultured hepatocytes. We found that the gluconeogenic effect of MKP-3 was more prominent in primary rat hepatocytes compared with Fao hepatoma cells. This difference may be due to the absence in the latter of expression of PGC-1 α , which is a key amplifier of gluconeogenesis. Interestingly, MKP-3 overexpression in primary hepatocytes significantly increased PGC-1 α expression. The effect of MKP-3 on PGC-1 α expression was not due to direct increase of *Pgc1a* transcription, since MKP-3 alone had no effect on transcription of the *Pgc1a* promoter and did not synergize with PGC-1 α to increase *Pepck* transcription (data not shown). Exclusion of ERK as the mediator of the insulin-antagonizing effect of MKP-3 on gluconeogenesis indicates that MKP-3 may have additional, yet-to-be-identified substrate(s) to mediate its gluconeogenic effect (7, 8). We identified FOXO1 to be such a candidate, supported by the following evidence: (a) MKP-3 interacts with and dephosphorylates FOXO1 on Ser256 directly in vitro. (b) MKP-3 reduces insulin-stimulated phosphorylation on Ser256 of FOXO1 and promotes FOXO1 nuclear translocation in Fao cells. (c) Endogenous MKP-3 can be co-immunoprecipitated with endogenous FOXO1, and the association is promoted by Dex but repressed by insulin. (d) Nuclear FOXO1 content is reduced and cytosolic FOXO1 phosphorylation on Ser256 is increased in the liver of lean mice upon MKP-3 knockdown. (e) MKP-3 has an additive effect specifically with FOXO1 but not with other accessory factors that can bind to *Pepck* and *G6pase* promoters to increase their transcription. MKP-3 also enhances FOXO1-activated transcription of the *Pgc1a* promoter. These results indicate that MKP-3 most likely increases transcription of gluconeogenic gene expression through activation of FOXO1. Our study demonstrates that MKP-3 has a role in regulating glucose metabolism in vivo and elucidates that FOXO1 is the downstream mediator of MKP-3 in promoting gluconeogenesis.

Our data together with previous studies allow us to integrate MKP-3 into the transcriptional network that controls gluconeogenesis in both physiological and pathological conditions. This is the first report to our knowledge identifying a phosphatase as a regulator of FOXO1 activity on initiation of the gluconeogenic program. The potential molecular mechanism of MKP-3-induced gluconeogenesis is summarized in Figure 7. The MKP-3 expression level is increased upon fasting by glucocorticoids or under an insulin-resistant state. Increased MKP-3 expression enhances FOXO1 transcriptional activity by dephosphorylating FOXO1 and promoting its nuclear translocation. Activation of FOXO1 increases PGC-1 α expression as well as that of the key gluconeogenic enzymes PEPCK and G6pase. PGC-1 α coactivates FOXO1 in *Pepck* and *G6pase* transcription, which in turn increases glucose output. Small molecule inhibitors of MKP-3 may be useful for attenuating obesity-related hyperglycemia.

Methods

Reagents and cells. PGC-1 α , PGC-1 α -Luc, HNF4 α , and COUP-TF expression plasmids were provided by Bruce M. Spiegelman (Dana Faber Cancer Institute). Flag-FOXO1 expression plasmid was provided by Akiyoshi Fukamizu (University of Tsukuba, Tsukuba, Japan). Ad-FOXO1 Δ 256 was provided by Henry Dong (University of Pittsburgh). Ad-shPGC-1 α , Ad-shFOXO1, and pcDNA-Flag-CRTC2 were provided by Marc Montminy (Salk Institute, La Jolla, California, USA). Ad-Flag-FOXO1 was provided by Pere Puigserver (Dana Farber Cancer Institute). PEPCK-Luc and mAF2-PEPCK-Luc were provided by Robert K. Hall and Daryl Granner (Vanderbilt University). G6Pase-Luc was provided by Richard M. O'Brien (Vanderbilt University). GFP-hFKHR was purchased from Addgene (21). Insulin, Dex, 8-bromo-cAMP, sodium pyruvate, and sodium lactate were purchased from Sigma-Aldrich. Primary rat hepatocytes were purchased from CellDirect Inc. and cultured according to the manufacturer's instructions. Glucagon was purchased from Novo Nordisk. D-[3- 3 H]-glucose and 2-[1- 14 C]-deoxy-D-glucose were purchased from PerkinElmer. Humulin R was purchased from Eli Lilly Inc. Antibodies for IR, IRS-1, MKP-3, Flag, phospho-tyrosine, PGC-1 α (immunoprecipitation), and anti-goat IgG-HRP were purchased from Santa Cruz Biotechnology Inc. ERK, Akt, phospho-ERK, phospho-Akt, FOXO1, phospho-FOXO1, and anti-mouse and anti-rabbit IgG-HRP antibodies were purchased from Cell Signaling Technology. PGC-1 α Western blotting antibody was purchased from Calbiochem. Tubulin antibody was purchased from Abcam.

Transfection of Fao cells and luciferase assay. Fao cells were transfected with FuGENE HD reagent (Roche Diagnostics) upon 50% confluence. The DNA/FuGENE HD ratio was 1:2.5. The *Renilla* luciferase expression plasmid was cotransfected as an internal control. Twenty-four hours after transfection, Fao cells were incubated overnight in serum-free RPMI 1640 medium. Forty-eight hours after transfection, cells were rinsed once in PBS and lysed in passive lysis buffer by 2 freeze-thaw cycles. Luciferase assay was performed using the Dual-Glo luciferase assay kit from Promega. The results were expressed as relative luciferase activity by normalizing firefly luciferase activity to *Renilla* luciferase activity.

RNA extraction and real-time PCR analysis. RNA samples were extracted using the TRIzol reagent from Invitrogen according to the manufacturer's manual. For real-time PCR analysis, random hexamers were used for reverse transcription. After reverse transcription, real-time PCR analysis was performed in a 15- μ l reaction in 96-well clear plates using Power SYBR Green RT-PCR Reagents Kit (Applied Biosystems) on ABI Prism thermal cycler model 7500 or Step-One Plus (Applied Biosystems). Reactions contained 1 \times reaction mix, 5.5 mM MgSO $_4$, 300 nM forward primer, 300 nM reverse primer, and SYBR green (Applied Biosystems). PCR conditions were: 50°C for 2 minutes, followed by 95°C for 10 minutes for 1 cycle, then 95°C for



15 seconds, followed by 60°C for 1 minute for 40 cycles. A dissociation stage was added after the PCR step to ensure the specificity of primers.

Glucose output assay. Primary rat hepatocytes were seeded in 12-well plates at 1.5 million/well in growth medium (William's E medium supplemented with 10% fetal bovine serum and cell maintenance supplement pack [Dex, insulin, transferrin, selenium complex, L-glutamine, and HEPES]). The next day, cells were transduced with adenoviruses expressing GFP, MKP-3 or shGFP, shMKP-3 at an MOI of 50. For PGC-1 α -knockdown experiments, Ad-GFP or Ad-MKP-3 was coinfecting with Ad-shScramble or Ad-shPGC-1 α at a ratio of 1:1. For FOXO1 loss-of-function experiments, Ad-GFP or Ad-MKP-3 was coinfecting with Ad-GFP or Ad-FOXO1 Δ 256 at a ratio of 1:0.4. Forty-eight hours after transduction, cells were washed 3 times with PBS and incubated in William's E medium containing 0.5% BSA, 1 μ M Dex, and 1 mM 8-bromo-cAMP for 5 hours. Cells were then incubated in 0.5 ml/well of phenol red-free, glucose-free DMEM containing 1 μ M Dex, 2 mM pyruvate, 20 mM lactate, and 1 mM 8-bromo-cAMP. Medium was collected 3 hours later and subjected to glucose measurement using the Amplex Red Glucose/Glucose Oxidase Assay Kit (Invitrogen). Cells were lysed, and protein concentration was determined for each lysate. The glucose output rate was normalized by cellular protein content.

Construction and purification of adenoviruses expressing MKP-3 and shRNA against MKP-3. The coding sequence of MKP-3 was amplified by PCR and cloned into the entry vector and the sequence confirmed. Then MKP-3 coding sequence was recombined into the Gateway-based pAd-CMV DEST vector (Invitrogen) according to the manufacturer's instructions. In order to construct adenoviral vectors expressing shRNAs against MKP-3, we designed 14 short hairpin oligonucleotides and complementary strands to target both rat and mouse MKP-3 or specifically for mouse MKP-3. The BLOCK-iT RNAi system (Invitrogen) was used for shRNA construction. Briefly, the top and bottom oligonucleotides were annealed and ligated into the Gateway-based pENTR/U6 vector (Invitrogen), and the sequence was confirmed. To evaluate the potency of these shRNAs in vitro, MKP-3 expression plasmid was cotransfected with the entry plasmids expressing MKP-3 shRNAs into HEK293A cells. Cells were harvested 48 hours later for testing of knockdown efficiency. In order to generate the recombinant adenovirus vectors expressing shRNAs for MKP-3, selected pENTR/U6-shRNA plasmids were recombined into the Gateway-based pAd-BLOCK-iT DEST vector (Invitrogen), according to the manufacturer's instructions. The MKP-3 shRNA used for in vitro study recognizes both rat and mouse sequence (GCCAATCT-GTTTGAGAAT); the MKP-3 shRNA used for in vivo study only recognizes the mouse sequence (GAACGATGCTTACGACATT). As a negative control, a recombinant adenovirus vector expressing an shRNA directed against GFP was generated. Amplification of recombinant adenovirus was performed according to the manufacturer's instructions (Invitrogen) using HEK 293A cells. Large-scale amplification and purification of recombinant adenoviruses were performed using the ViraBind Adenovirus Purification Kit according to the manufacturer's instructions (Cell Biolabs Inc.).

Immunoprecipitation and Western blot analysis. To prepare cell lysates, primary rat hepatocytes and Fao cells were washed with ice-cold PBS once and lysed with lysis buffer supplemented with protease inhibitors. To prepare liver lysates, livers were immediately frozen in liquid nitrogen and pulverized into powder, and approximately 100 mg was used for homogenization in lysis buffer supplemented with protease inhibitors. To immunoprecipitate endogenous MKP-3 from cell or liver lysates, 30 μ l of Exactra D immunoprecipitation matrix (Santa Cruz Biotechnology Inc.) slurry was used to pre-clear cell or liver lysates at 4°C for 30 minutes. Then 40 μ l of MKP-3 antibody-bound Exactra D immunoprecipitation matrix slurry was added to pull down MKP-3. To immunoprecipitate Flag-FOXO1 from Fao cell lysates, 30 μ l of protein A/G immunoprecipitation matrix slurry was used to pre-clear protein lysates. Following addition of anti-Flag antibody

and 1 hour incubation at 4°C, 40 μ l of protein A/G immunoprecipitation matrix slurry was added to pull down Flag-FOXO1 captured by anti-Flag antibody. To immunoprecipitate PGC-1 α , 900 μ g of protein prepared from primary hepatocytes was incubated with 1 μ g of PGC-1 α antibody at 4°C overnight. The next day, 60 μ l of protein A bead slurry was added and incubated at 4°C for 4 hours. For direct Western blot analysis of MKP-3 expression, ERK phosphorylation, and tubulin loading control, 100 μ g of cell or liver lysates from each sample were used. Following PAGE on 4%-12% gel (Bio-Rad), the resolved proteins were transferred onto PVDF membranes. Membranes were blocked in 1% BSA/1 \times TBST or 5% milk/1 \times TBST for 1 hour, then incubated with the appropriate primary antibodies in the presence of 1% BSA/1 \times TBST or 5% milk/1 \times TBST, followed by incubation with appropriate HRP-linked secondary antibodies for 1 hour in 5% milk/1 \times TBST. Protein bands were detected by ECL Western blotting detection reagent (PerkinElmer).

GST pull-down assay. GST-MKP-3 and GST-FOXO1 fusion proteins were purified using the Bulk GST Purification Module kit (GE Healthcare/Amersham Biosciences) according to the manufacturer's instructions. GST-MKP-3 (5.0 μ g) and GST-FOXO1 (5.0 μ g) were incubated overnight at 4°C. Twenty microliters of respective antibody (200 μ g/ml MKP-3 antibody and 100 μ g/ml FOXO1 antibody) or control IgG was added and incubated for 8 hours at 4°C with gentle rocking. The immune complexes were collected by addition of 30 μ l of protein A/G-agarose beads and incubation for 4 hours at 4°C, followed by centrifugation. Precipitates were washed 4 times with 1 \times wash buffer (20 mM HEPES pH 7.6, 50 mM KCl, 1 mM DTT, 0.25% Nonidet P40, 5 mM NaF, 1 mM EGTA, 5 mM MgCl₂, 0.25 mM PMSF) and 2 times with 1 \times PBS, and the immunoprecipitated complexes were suspended in SDS sample buffer and analyzed by SDS-PAGE followed by Western blot analysis (22).

ChIP assay. ChIP assays were performed with the Chromatin Immunoprecipitation System according to the manufacturer's instructions (Invitrogen). Fao hepatocytes were transduced with adenovirus expressing either MKP-3 or GFP for 48 hours. Then cells were treated with RPMI 1640 medium plus 1 μ M Dex and 1 mM cAMP for 6 hours. After treatment, cells were fixed with formaldehyde for 10 minutes at room temperature. Then cells were lysed and sonicated. Soluble chromatin was co-immunoprecipitated with antibody against FOXO1 (Cell Signaling Technology) or IgG. The crosslinked DNA samples were subjected to PCR with the following primers: PEPCCK, 5'-GTTTCACGTCTCAGAGCTGA-3' and 5'-ACCGTGACTGTTGCTGATGC-3'; G6Pase, 5'-CAGACTCTGCCCTGAGCCTCTGGCCTG-3' and 5'-CCCTGGATTTCAGTCTGTAGGTCAACCTAGC-3'.

In vitro dephosphorylation. Fao cells were incubated in serum-free RPMI 1640 medium overnight. The next day, Fao cells were incubated for another 3 hours in serum-free and glucose-free medium in the presence of 1 μ M Dex, 2 mM pyruvate, and 20 mM lactate. Insulin was added for the last 15 minutes. Endogenous FOXO1 was immunoprecipitated using FOXO1 antibody from Fao cells and mixed with immunoprecipitated GFP or MKP-3 protein prepared from Fao cells expressing GFP or MKP-3 via adenovirus-mediated gene transfer. The IP mixtures were washed 3 times with lysis buffer first, then washed 3 times with phosphatase buffer (50 mM HEPES, pH 7.5, 150 mM NaCl, 1 mM EDTA, 5 mM DTT, 0.1 mg/ml BSA, 3% DMSO). Then, the IP complexes were incubated in phosphatase buffer for 4 hours at room temperature with gentle shaking. At the end of incubation, IP complexes were centrifuged at 13,400 g for 2 minutes at 4°C. The phosphatase buffer was removed, and immunoprecipitation matrix was boiled in 2 \times protein loading buffer.

Liver fractionation. A small sample of liver of roughly 0.7-cm diameter was collected and put into pre-chilled 1 ml Downs homogenizer, and 1 ml of cold buffer A was added (25 mM Tris-Cl, pH 7.5, 50 mM KCl, 2 mM MgCl₂, 1 mM EDTA, freshly added DTT to a final concentration of 5 mM, and freshly added protease inhibitor cocktail). Liver was homogenized on ice with 2 loose



strokes, followed by 10 tight strokes. Liver homogenate was then transferred to a 1.5-ml tube and spun at 2,300 g for 10 minutes at 4°C. The supernatant (cytosol) was transferred to a new 1.5-ml tube and frozen at -80°C. The pellet was rinsed in 1 ml buffer A and spun at 2,300 g for 10 minutes at 4°C. The supernatant was aspirated, and nuclear protein was extracted by addition of an appropriate amount of buffer B (25 mM Tris-Cl, pH 7.5, 0.42 M NaCl, 1.5 mM MgCl₂, 0.5 mM EDTA, 25% sucrose, freshly added DTT to a final concentration of 1 mM, and freshly added protease inhibitor cocktail). The nuclear pellet was resuspended in buffer B and kept on ice for 30 minutes. The solution was then sonicated twice for 10 seconds each (about 90–95 W) and spun at 13,400 g for 10 minutes at 4°C. The supernatant (nuclear extract) was transferred to a new 1.5-ml tube and frozen at -80°C.

Mouse models and administration of adenoviruses. For all animal experiments, mice were randomized into experimental groups with equal body weight and postprandial blood glucose levels. To establish the DIO model, male C57BL/6J mice were purchased from The Jackson Laboratory at 3 weeks of age, acclimated for a week, and fed either a chow diet (5% kcal from fat) or a high-fat diet (60% kcal from fat; Research Diets Inc.) for 16–30 weeks. Blood glucose levels were measured using a glucometer. Plasma insulin levels were measured by ELISA (ALPCO Diagnostics). For pyruvate challenge, mice were fasted overnight and injected with sodium pyruvate at a dose of 2 g/kg for lean mice and 1 g/kg for DIO mice. For glucose tolerance tests, mice were fasted overnight, and glucose was injected at a dose of 2 g/kg for lean mice and 1 g/kg for DIO mice. For insulin tolerance tests, mice were fasted for 6 hours, and insulin was injected at a dose of 0.5 U/kg for lean mice and 0.75 U/kg for DIO mice. Experiments were performed 6–13 days after virus injection. Animal experiments were approved by the Institutional Animal Care and Use Committee of Rhode Island Hospital.

Hyperinsulinemic-euglycemic clamp study. The right jugular vein of DIO mice was catheterized. One week following surgery, adenoviruses expressing shGFP or shMKP-3 were injected. Seven to 13 days after injection, hyperinsulinemic-euglycemic clamps were performed. After an overnight fast, HPLC-purified d-[3-³H]-glucose (0.05 μCi/min) was infused during the 2-hour basal period, and blood samples were collected at 60 and 120 minutes to estimate the rate of basal hepatic glucose production. After the

basal period, a 3-minute infusion of a bolus of insulin was performed, and then a 120-minute hyperinsulinemic-euglycemic clamp was conducted with a primed-continuous infusion of human insulin (Humulin R). Blood samples were collected at 10-minute intervals for the immediate measurement of plasma glucose concentration, and 25% glucose solution was infused at variable rates to maintain plasma glucose at basal concentrations. All infusions were performed using microdialysis pumps (CMA/Microdialysis). Blood samples were taken at 80, 85, 90, 100, 110, and 120 minutes after the start of clamps for the determination of plasma [³H]glucose and ³H₂O concentrations.

Statistics. Results are expressed as mean ± SEM. Unpaired 2-tailed Student's *t* test was used to compare differences between groups. Statistical significance was indicated when the *P* value was less than 0.05.

Acknowledgments

The authors thank Bruce Spiegelman, Pere Puigserver, Akiyoshi Fukamizu, Henry Dong, Marc Montminy, Robert K. Hall, Daryl Granner, and Richard M. O'Brien for providing the reagents used in this study. The authors also thank Mary Chan for proofreading the manuscript. This work was supported by a Child Health Research grant from the Charles H. Hood Foundation; by a Lifespan Developmental Grant from Rhode Island Hospital; and by NIDDK grants R01 DK080746 grant (to H. Xu) and R01 DK072230 (to G. Xiao).

Received for publication April 6, 2010, and accepted in revised form August 18, 2010.

Address correspondence to: Zhidan Wu, Cardiovascular and Metabolism, Novartis Institutes for BioMedical Research, 100 Technology Square, Cambridge, Massachusetts 02139, USA. Phone: 617.871.7345; Fax: 617.871.7051; E-mail: zhidan.wu@novartis.com. Or to: Haiyan Xu, Hallett Center for Diabetes and Endocrinology, Brown Medical School, 55 Claverick St., Rm 318, Providence, Rhode Island 02903, USA. Phone: 401.444.0347; Fax: 401.444.3784; E-mail: hxu@lifespan.org.

1. Saltiel AR, Kahn CR. Insulin signalling and the regulation of glucose and lipid metabolism. *Nature*. 2001;414(6865):799–806.
2. Myers MG Jr, White MF. Insulin signal transduction and the IRS proteins. *Annu Rev Pharmacol Toxicol*. 1996;36:615–658.
3. Holman GD, Kasuga M. From receptor to transporter: insulin signalling to glucose transport. *Diabetologia*. 1997;40(9):991–1003.
4. Pilakis SJ, Granner DK. Molecular physiology of the regulation of hepatic gluconeogenesis and glycolysis. *Annu Rev Physiol*. 1992;54:885–909.
5. Vidal-Puig A, O'Rahilly S. Metabolism. Controlling the glucose factory. *Nature*. 2001;413(6852):125–126.
6. Sutherland C, O'Brien RM, Granner DK. Phosphatidylinositol 3-kinase, but not p70/p85 ribosomal S6 protein kinase, is required for the regulation of phosphoenolpyruvate carboxykinase (PEPCK) gene expression by insulin. Dissociation of signaling pathways for insulin and phorbol ester regulation of PEPCK gene expression. *J Biol Chem*. 1995;270(26):15501–15506.
7. Sutherland C, Waltner-Law M, Gnudi L, Kahn BB, Granner DK. Activation of the ras mitogen-activated protein kinase-ribosomal protein kinase pathway is not required for the repression of phosphoenolpyruvate carboxykinase gene transcription by insulin. *J Biol Chem*. 1998;273(6):3198–3204.
8. Gabbay RA, et al. Insulin regulation of phosphoenolpyruvate carboxykinase gene expression does not require activation of the Ras/mitogen-activated protein kinase signaling pathway. *J Biol Chem*. 1996; 271(4):1890–1897.
9. Liao J, Barthel A, Nakatani K, Roth RA. Activation of protein kinase B/Akt is sufficient to repress the glucocorticoid and cAMP induction of phosphoenolpyruvate carboxykinase gene. *J Biol Chem*. 1998; 273(42):27320–27324.
10. Schmoll D, et al. Regulation of glucose-6-phosphatase gene expression by protein kinase Balpha and the forkhead transcription factor FKHR. Evidence for insulin response unit-dependent and -independent effects of insulin on promoter activity. *J Biol Chem*. 2000;275(46):36324–36333.
11. Wolfrum C, Asilmaz E, Luca E, Friedman JM, Stoffel M. Foxa2 regulates lipid metabolism and ketogenesis in the liver during fasting and in diabetes. *Nature*. 2004;432(7020):1027–1032.
12. Puigserver P, et al. Insulin-regulated hepatic gluconeogenesis through FOXO1-PGC-1alpha interaction. *Nature*. 2003;423(6939):550–555.
13. Reynolds RM, et al. Altered control of cortisol secretion in adult men with low birth weight and cardiovascular risk factors. *J Clin Endocrinol Metab*. 2001; 86(1):245–250.
14. Andrew R, Phillips DI, Walker BR. Obesity and gender influence cortisol secretion and metabolism in man. *J Clin Endocrinol Metab*. 1998;83(5):1806–1809.
15. Rhee J, et al. Regulation of hepatic fasting response by PPARgamma coactivator-1alpha (PGC-1): requirement for hepatocyte nuclear factor 4alpha in gluconeogenesis. *Proc Natl Acad Sci U S A*. 2003; 100(7):4012–4017.
16. Daitoku H, Yamagata K, Matsuzaki H, Hatta M, Fukamizu A. Regulation of PGC-1 promoter activity by protein kinase B and the forkhead transcription factor FKHR. *Diabetes*. 2003;52(3):642–649.
17. Xu H, et al. Dual specificity MAP kinase phosphatase 3 activates PEPCK and increases gluconeogenesis in rat hepatoma cells. *J Biol Chem*. 2005;280(43):36013–36018.
18. Van Der Heide LP, Hoekman MF, Smidt MP. The ins and outs of FoxO shuttling: mechanisms of FoxO translocation and transcriptional regulation. *Biochem J*. 2004;380(pt 2):297–309.
19. Schmoll D, Grempler R, Barthel A, Joost HG, Walther R. Phorbol ester-induced activation of mitogen-activated protein kinase/extracellular-signal-regulated kinase kinase and extracellular-signal-regulated protein kinase decreases glucose-6-phosphatase gene expression. *Biochem J*. 2001;357(pt 3):867–873.
20. Rodriguez A, et al. Mature-onset obesity and insulin resistance in mice deficient in the signaling adapter p62. *Cell Metab*. 2006;3(3):211–222.
21. Nakamura N, Ramaswamy S, Vazquez F, Signoretti S, Loda M, Sellers WR. Forkhead transcription factors are critical effectors of cell death and cell cycle arrest downstream of PTEN. *Mol Cell Biol*. 2000; 20(23):8969–8982.
22. Yu S, et al. General transcription factor IIA-gamma increases osteoblast-specific osteocalcin gene expression via activating transcription factor 4 and runt-related transcription factor 2. *J Biol Chem*. 2008; 283(9):5542–5553.